

Numerical Predictions on the Wake Interference Flow in Two-dimensional Street Canyon based on Various RANS Turbulence Closure Models

Mohd Hilman Mohd Akil Tan^{1, 2}, Mohd Faizal Mohamad^{2,3*}, Azli Abd Razak², Nurnida Elmira Othman², Shahliza Azreen Sarmin⁴

¹Faculty of Engineering, Built Environment & Information Technology, SEGi University, 47810 Petaling Jaya, Selangor, Malaysia ²Wind Engineering & Building Physics (WEBP), Faculty of Mechanical Engineering, Universiti Teknologi MARA, 40450 Shah Alam, Selangor, Malaysia

³Smart Manufacturing Research Institute (SMRI), Universiti Teknologi MARA, 40450 Shah Alam, Selangor, Malaysia ⁴Universiti Kuala Lumpur, Malaysian Institute of Aviation Technology, 43800 Dengkil, Selangor, Malaysia ^{*}corresponding author: faizal3744@uitm.edu.my

ABSTRACT

The precise numerical prediction of urban flow patterns is crucial for evaluating ventilation performance, pollution dispersion, and pedestrian comfort in densely built environments. Among these types of patterns, the wake interference flow poses a distinct modeling difficulty due to its complex vortex dynamics. This study performed a series of steady Reynolds-Averaged Navier-Stokes (RANS) simulations to evaluate the predictive efficiency of five turbulence closure models: standard k-ε (STD), renormalisation group k-ε (RNG), realizable k-ε (RLZ), shear-stress transport k-ω (SST), and Reynolds stress model (RSM) in a two-dimensional (2D) idealized street canyon with an aspect ratio of 3 within the wake interference flow regime. The predicted results were compared with wind tunnel experimental data using velocity profiles, statistical validation metrics, and streamlines visualization. The results demonstrate that the quantitative assessment utilizing the factor of two observations (FAC2) distinctly revealed a satisfactory predicted of streamwise velocity within the street canyon, topped by RNG (0.92) and followed by STD (0.91), RSM (0.90), SST (0.89), and RLZ (0.88). Nevertheless, all models inadequately predicted the vertical velocity, as the FAC2 values fell below the threshold of 0.5. The qualitative assessment of the velocity streamlines indicates that the RNG and STD predictions closely resembled the flow pattern obtained from the experimental results that determine the main characteristics of the wake interference flow regime. Other models exhibited inadequate performance due to the observation of completely different flow patterns. Consequently, it can be concluded that while all models can estimate the streamwise velocity in the wake interference regime with good accuracy, substantial constraints persist in predicting the in-canyon vertical velocity. The observed limitations, together with the apparent variation between models in replicating secondary vortex formations, suggest several avenues for future investigations.

Keywords: Wake interference flow; street canyon; RANS; urban ventilation; wind environment

Nomenclature

u Streamwise velocity u_{ref} Reference velocity w Vertical velocity

k Turbulent kinetic energy

k- ε k-epsilon k- ω k-omega

Abbreviations

CFD Computational fluid dynamics RANS Reynolds-averaged Navier-Stokes

STD Standard k-e

RNG Renormalisation group k-ε

RLZ Realizable k-ε

SST Shear-stress transport k-ω RSM Reynolds stress model

Received on 18.08.2025 Accepted on 01.10.2025 Published on 03.10.2025

1.0 INTRODUCTION

The accurate prediction of airflow patterns in urban environments is essential for addressing environmental concerns such as pollutant dispersion, thermal comfort, and energy efficiency. Street canyons, defined as roads flanked by buildings on both sides, have garnered significant attention due to their tendency to trap pollutants and influence microclimates. The aerodynamic behaviour in street canyons is influenced by several factors, including the aspect ratio (the ratio of street width, S to building height, H) [1–3], building morphology [4–7], and roof configuration [8–11]. Oke [4] identified three characteristic flow regimes based on aspect ratio: skimming flow, wake interference flow, and isolated roughness flow. In skimming flow (typically when the aspect ratio S/H < 1.2), the main stream flows over the canyon with limited interaction, while the canyon itself exhibits a stable recirculation vortex. Wake interference flow (1.2 < S/H < 5.0) occurs when the downstream of windward building façade enhances downward momentum, resulting in complex secondary flows within the canyon. In isolated roughness flow (S/H > 5.0), buildings are widely spaced, allowing the flow around each to behave more independently, with limited interaction between wakes.

Wind tunnel experiments have proven effective in replicating urban flow conditions under controlled environments. These setups offer high reproducibility and enable isolated analysis of key parameters such as wind direction, speed, and geometry. Additionally, integration with techniques like particle image velocimetry (PIV) provides detailed visualization of airflow structures within the canyon [12–14]. However, the wind tunnel approach faces limitations, primarily due to scaling effects that hinder accurate representation of full-scale Reynolds numbers. Physical models are often simplified, lacking the detailed architectural features of real urban structures, and measurement techniques may struggle to resolve near-wall flows accurately. Moreover, wind tunnel testing is often costly and time-consuming, limiting its broader application.

In contrast, computational fluid dynamics (CFD) has become increasingly popular for studying urban airflow and pollutant dispersion, thanks to improvements in computational power and modeling techniques. Advanced turbulence models such as large-eddy simulation (LES) and detached eddy simulation (DES) offer high-fidelity predictions and have shown good agreement with experimental data. Nevertheless, these methods are computationally intensive and demand careful definition of boundary conditions, especially at the inlet and near-wall regions. For practical engineering applications, the Reynolds-Averaged Navier-Stokes (RANS) approach remains a widely used and more computationally efficient alternative. While RANS may not capture transient flow features as accurately as LES or DES, its balance between computational cost and predictive capability, particularly when paired with suitable turbulence closure models. The RANS turbulence closure models are an attractive choice for urban airflow studies where fine-scale turbulence details are often less critical than overall flow [15–17].

While CFD has become an essential tool for analysing urban airflow, the accuracy of its predictions is strongly influenced by the choice of turbulence closure models, particularly within the RANS framework. RANS models are computationally efficient and practical for urban simulations; however, their capability to reproduce detailed flow structures within street canyons remains limited. Several previous studies have extensively examined RANS model performance under skimming flow regime by applying renormalization group k- ε (RNG), realizable k- ε (RLZ), standard k- ε (STD) and shear stress transport k- ω (SST) [6,18–22]. Streamwise velocity in the canyon was found to be in good agreement with wind tunnel data; however, there is a considerable overprediction in the vertical velocity near the windward wall [6]. Comparable findings have been documented by the application of LES, indicating that additional investigations are necessary to clarify the cause of the discrepancy [23]. Furthermore, in the scenario of isolated roughness flow, the comparison of simulated results is limited, as an increased distance between buildings requires measuring more data points to achieve greater accuracy, thus increasing the time required for the experiment and making it a challenging task.

However, less attention has been given to the wake interference flow regime, which presents a more complex aerodynamic environment due to strong interactions between upstream and downstream building wakes and the presence of multiple in-canyon vortices. These dynamics pose significant challenges for RANS-based models, which often struggle to capture unsteady features and momentum exchanges that dominate this regime. The limitations in the current model performance under wake interference conditions highlight the need for further evaluation and model validation. In Malaysia, terraced housing configurations which are characterized by long buildings facing one another and separated by aspect ratio that fall within this flow regime continue to receive less attention [24,25]. The rising number of automobiles in residential areas may adversely affect pollution dispersion owing to traffic-related sources. Thus, it is crucial that this study offer insights that help advance knowledge of building design, pollution control, and urban planning.

In response to this gap, the present study aims to systematically assess the performance of various RANS turbulence closure models including the standard k- ϵ (STD), realizable k- ϵ (RLZ), renormalization group k- ϵ (RNG), shear stress transport k- ω (SST) and Reynolds Stress Model (RSM) in predicting the flow patterns within a two-dimensional street canyon under the wake interference flow regime. By comparing simulation results against wind tunnel measurements, this study seeks to identify the turbulence model that best captures key flow features such as primary recirculation vortex, secondary vortices and and vertical exchange processes. The

outcomes are expected to support more accurate and computationally efficient modeling strategies for urban environmental applications involving complex flow regimes.

2.0 METHODOLOGY

2.1 Building Configuration and Computational Domain

The simulations are conducted through the computational domain depicted in Fig. 1(a), which consists four idealized 2D street canyons. Each building comprises a cross-section of 0.2 (width, W) × 0.2 (height, H) m² and is separated by a street canyon that establishes the aspect ratio S, defined as the ratio of street width to building height, equal to 3H. The domain dimensions are established as 12H in the streamwise direction, 2H in the spanwise direction, and 3H and 3H in the vertical direction. Figure 1(b) displays the five measurement lines in the vertical manner at x/H = -1.0, -0.5, 0.0, 0.5 and 1.0 in the target canyon.

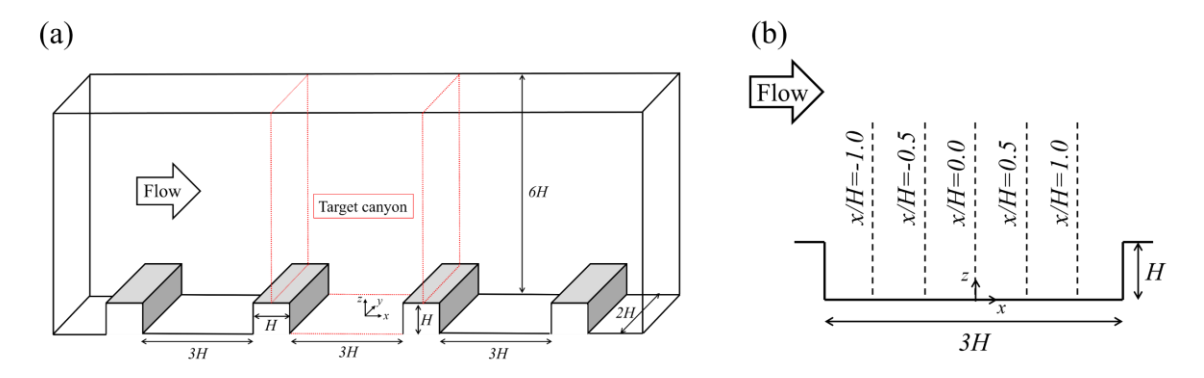


Figure 1. Schematic representation of the (a) simulation domain and (b) measurement lines within the target canyon at v/H = 0.0.

2.2 Boundary Conditions and Solver Settings

Cyclic boundary conditions are adopted for both the streamwise and spanwise directions, simulating the infinitely repeated street canyon. The flow is driven by an additional momentum source included in the RANS equations to attain a cross section average velocity 10.0 m/s. The top domain is assigned as slip conditions, whilst the building and floor surfaces are defined as no-slip conditions employing standard wall functions. The open-source software Open Field Operation and Manipulation (OpenFOAM) [28] is employed for three dimensional (3D) steady Reynolds-Averaged Navier-Stokes (RANS) simulations. Five turbulence closure models are evaluated for solving the RANS equations: standard k- ϵ (STD) [29], renormalization group k- ϵ (RNG) [30], realizable k- ϵ (RLZ) [31], shear stress transport k- ω (SST) [32], and Reynolds Stress Model (RSM) [33]. The governing equations are solved through the Semi-Implicit Method for Pressure-Linked Equations (SIMPLE) algorithm. Second-order linear interpolation is utilized for the gradient terms, and second-order discretization schemes are applied to both the convection and viscous terms of the governing equations. The convergence of the simulation is assessed by setting minimal residual thresholds of 10^{-5} for pressure and 10^{-6} for the other equations.

3.0 RESULTS AND DISCUSSION

3.1 Grid Sensitivity Analysis

The grid sensitivity study utilizes the RNG as the closure model, with the domain discretized into a structured hexahedral mesh that facilitates accurate resolution of flow characteristics within the urban canopy and shear flow region. The grid size is defined as a function of building height H: H/10 (coarse), H/20 (medium), and H/40 (fine) in the streamwise and spanwise directions, while the vertical direction is limited to a height of 2H [24]. The grid density is adjusted after the 2H height by keeping the stretching ratio below 1.3 in the vertical direction. This results in 138,000, 912,000, and 4,992,000 meshes for coarse, medium, and fine grids, respectively. The H/10 coarse mesh is chosen in accordance with the requirement that each building side use a minimum of 10 cells [34]. In the grid independence study, the medium mesh is discretized to H/20 and the fine mesh to H/40, compared to the coarse mesh following the standard best practice where grids are systematically refined by factor of 2 [35].

Figure 2 shows the dimensionless streamwise velocity u/u_{ref} along five vertical lines at x/H = -1.0, -0.5, 0.0, 0.5, and 1.0 in the x-z plane at y/H = 0.0. Both height z and velocity u are made dimensionless with the building height H and the reference velocity u_{ref} at a height of 2H, measured at the middle of the target canyon. In the canyon's upstream area (x/H = -1.0 and -0.5), medium and fine grids show consistent predictions both inside and outside the canyon. The coarse grid shows the limitations in predicting the near wall viscous flow zone by underpredicting the flow near the canyon bottom. At the centre of the canyon (x/H = 0.0), no significant differences are observed over any mesh sizes. Furthermore, in the downstream region of the canyon where horizontal

momentum is significant, all grid sizes yield comparable predictions, except near the canyon floor, given that the coarse grid underestimates the velocity magnitude.

Figure 3 presents the dimensionless vertical velocity along five vertical lines at x/H = -1.0, -0.5, 0.0, 0.5, and 1.0 in the x-z plane at y/H = 0. Within the upstream region of the street canyon, the coarse grid shows reduced accuracy in predicting vertical velocity components compared to the medium and fine grid configurations, as clearly illustrated at positions x/H = -1.0 and -0.5. Above the building height z/H = 1.0, all three grid resolutions show nearly identical results.

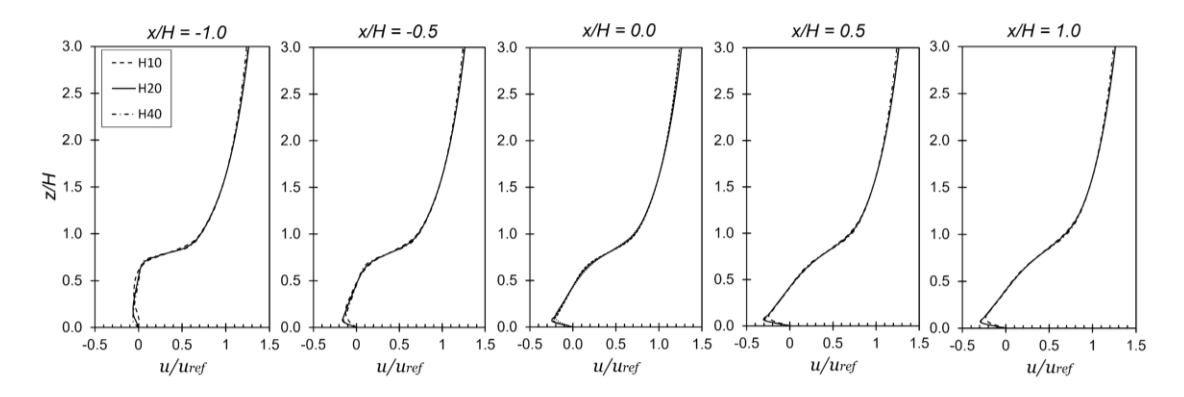


Figure 2. Grid sensitivity analysis: Dimensionless streamwise velocity over the three different grids, coarse (H/10): dotted line, medium (H/20): solid line and fine (H/40): dashed line along seven vertical lines x/H = -1.0, -0.5, 0.0, 0.5 and 1.0.

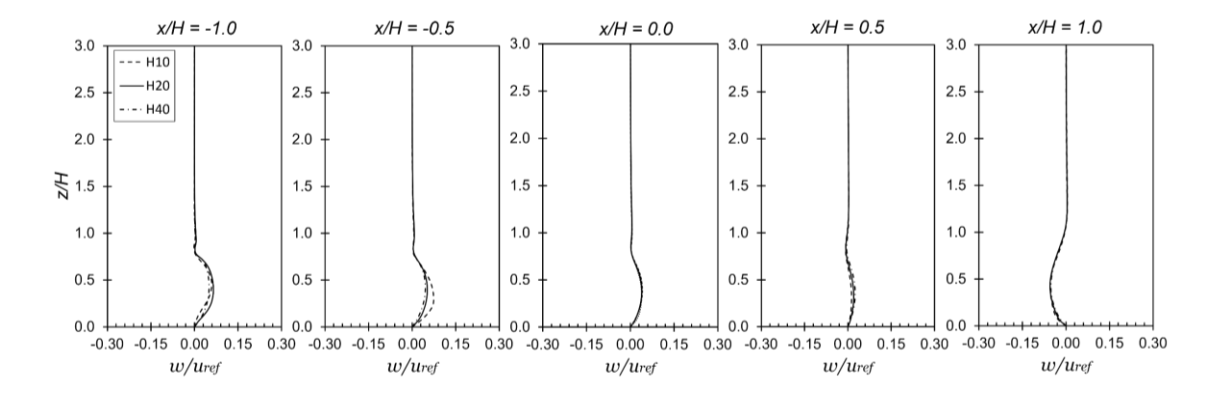


Figure 3. Grid sensitivity analysis: Dimensionless vertical velocity comparison on the three different grids, coarse (H/10): dotted line, medium (H/20): solid line and fine (H/40): dashed line along five vertical lines x/H = -1.0, -0.5, 0.0, 0.5 and 1.0.

Furthermore, the grid convergence index (GCI) [35] is employed to quantitatively evaluate the reliance of the grids on the solutions, as shown by Eq. (1).

$$GCI_{medium} = F_s \left| \frac{r^p \left[\left(u_{medium} / u_{ref} - u_{fine} / u_{ref} \right) \right]}{1 - r^p} \right| \tag{1}$$

In this equation, $F_s = 1.25$ represents the safety factor, as three computational grids are employed for the analysis; r denotes the linear grid refinement, which is $\sqrt{2}$ and p, the formal order of accuracy, is 2, indicating the usage of second-order discretisation schemes.

Figure 4 and Figure 5 show the GCI for the streamwise velocity and vertical velocity, respectively to quantitatively estimate the error of the medium grid towards the fine grid at the five vertical lines at x/H = -1.0, -0.5, 0.0, 0.5, and 1.0. It has been confirmed that for every line under evaluation, the average GCI values for both velocity components remain below 1%. Therefore, it indicates that the medium mesh could provide sufficient resolution in capturing the flow features while achieving the grid independent results. It also ensure the reliability

of the numerical solution without the need for further mesh refinement. Hence, the medium mesh configuration is selected to be used for all the subsequent simulations.

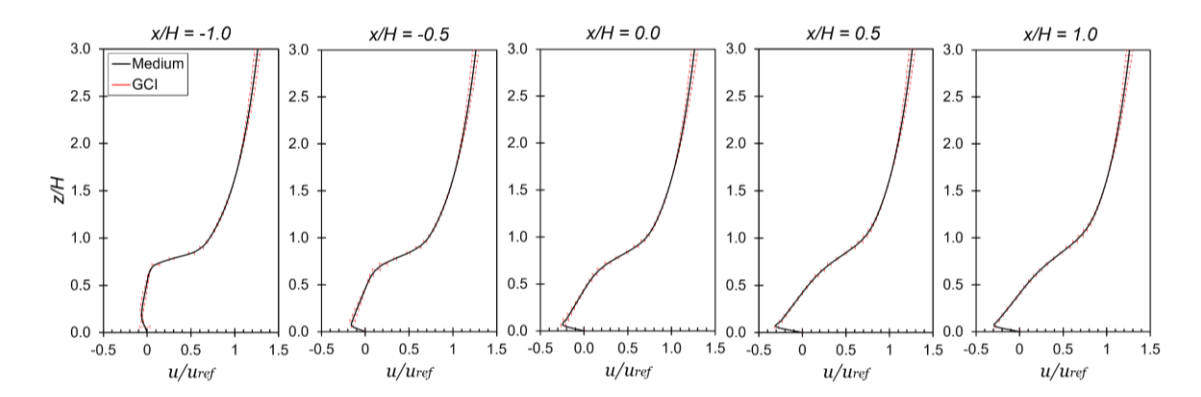


Figure 4. The grid convergence index (GCI) for streamwise velocity at the designated locations x/H = -1.0, -0.5, 0.0, 0.5, and 1.0 for medium grid.

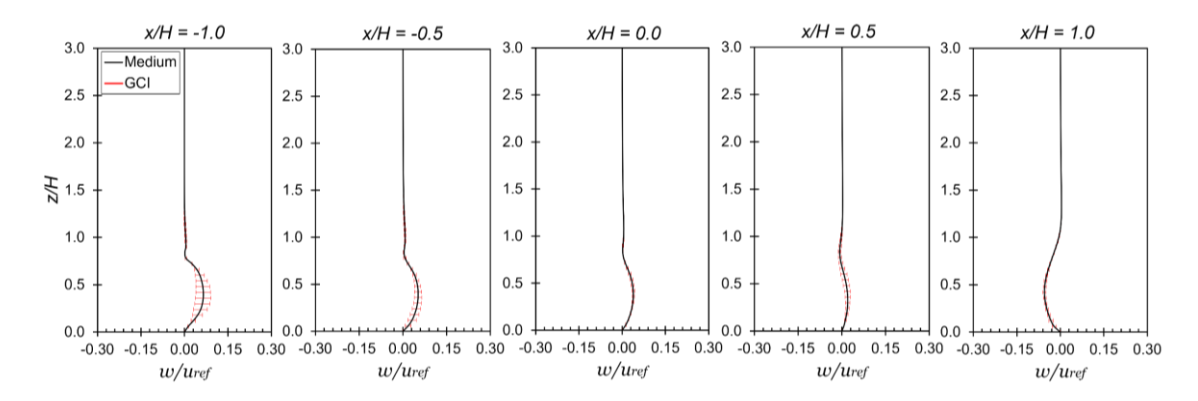


Figure 5. The grid convergence index (GCI) for vertical velocity at the designated locations x/H = -1.0, -0.5, 0.0, 0.5, and 1.0 for medium grid.

3.2 Flow fields of various closure models

3.2.1 Velocity Profiles

The velocity profiles from the simulations of all closure models are compared with the wind tunnel data (EXP) [36]. The experiments are performed in a closed-circuit wind tunnel with a test section of 8.0 m in length, 1.5 m in width, and 1.0 m in height. The two-dimensional (2D) street canyons are represented by positioning 40 horizontally elongated bars with a cross-section of 25 mm × 25 mm across the width of the tunnel's floor. The assessment of streamwise and vertical velocities is conducted utilizing particle image velocimetry (PIV) with a 1.8 mm thick laser light sheet emitted from beneath the tunnel floor. Furthermore, the charge-coupled device (CCD) camera captures images at a frequency of 1000 Hz.

The comparison of the streamwise and vertical velocity components obtained from simulations with the experimental data are shown in Figures 6 and 7, respectively. The dimensionless streamwise velocity (u/u_{ref}) is shown in Figure 6 for five different locations at x/H = -1.0, -0.5, 0.0, 0.5 and 1.0. The streamwise profiles predicted by all models at the position adjacent to the leeward façade (x/H = -1.0) mostly are consistent with experimental data, despite minor variations observed for the STD near the ground (z/H < 0.5). At x/H = -0.5, STD and RNG demonstrate a pronounced reverse flow in the region z/H < 0.5, aligning closely with the experimental results and exhibiting similar profile trends. Three other models (RLZ, SST, and RSM) poorly estimate the velocity profiles, as reverse flow does not occur in the vicinity of the ground region. At the canyon center (x/H = 0.0), SST and RSM fail to accurately predict the reverse flow near the wall, whereas other models (STD, RNG, and RLZ) successfully replicate the phenomenon with comparable accuracy. Furthermore, in the windward area (x/H = 0.5 and 1.0), where horizontal momentum is higher, all models demonstrate an excellent ability for accurate flow prediction within the canyon height.

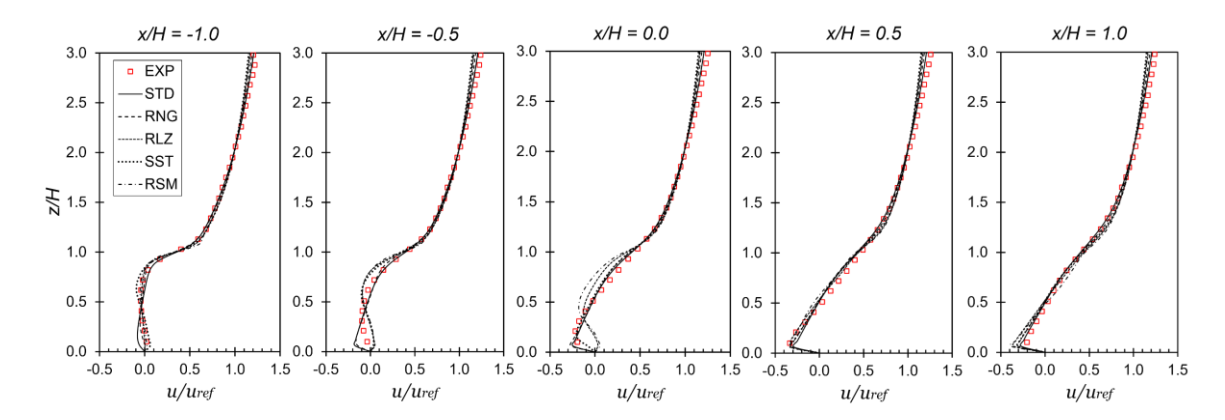


Figure 6. Comparison of dimensionless streamwise velocity (u/u_{ref}) obtained from RANS simulations of various closure models with wind-tunnel results along five vertical lines of the target canyon at (a) x/H = -1.0, -0.5, 0.0, 0.5 and 1.0.

Figure 7 shows the comparison of dimensionless vertical velocity w/u_{ref} obtained from the simulations and wind tunnel measurements at x/H = -1.0, -0.5, 0.0, 0.5 and 1.0. At x/H = -1.0, within the canyon height, STD and RNG overestimate the upward velocity whereas RLZ, SST and RSM depict weak velocity magnitude with nearly zero values up to mid-height of the canyon. At x/H = -0.5, STD, RNG, and SST demonstrate a close prediction of the upward flow; however, RLZ and RSM predict an entirely opposite flow direction. Additionally, when x/H =0.0, only the SST model shows predictive ability in comparison to the experimental data, while other models show overestimation and underprediction with STD accounting for the weakest velocity. Furthermore, when x/H = 0.5, RLZ and RSM substantially overestimate the upward flow, gradually diminishing until $z/H \approx 1.5$. On the other hand, the STD prediction is closer, with some minor discrepancies close to the wall region. At x/H = 1.0, the predictions of models RLZ and RSM are substantially consistent with the experimental data, but other models exhibit significant underprediction for the downward flow. It can be concluded that, for the velocity profiles over the canyon height z/H > 1.0, all models predict both vertical and streamwise components accurately. The discrepancies in predicting the velocity profiles within the canyon height (z/H < 1.0) may be attributed to the inability of RANS models to replicate the separation at the roof level, which generates primary recirculation and secondary corner vortices, resulting in high strain rates and strongly anisotropic turbulence (see Figure 9). RANS models frequently approximate turbulence as locally isotropic based on the Boussinesq eddy viscosity assumption, hence inaccurately predicting momentum transfer and vertical velocity in regions dominated by anisotropic rapid strain [37].

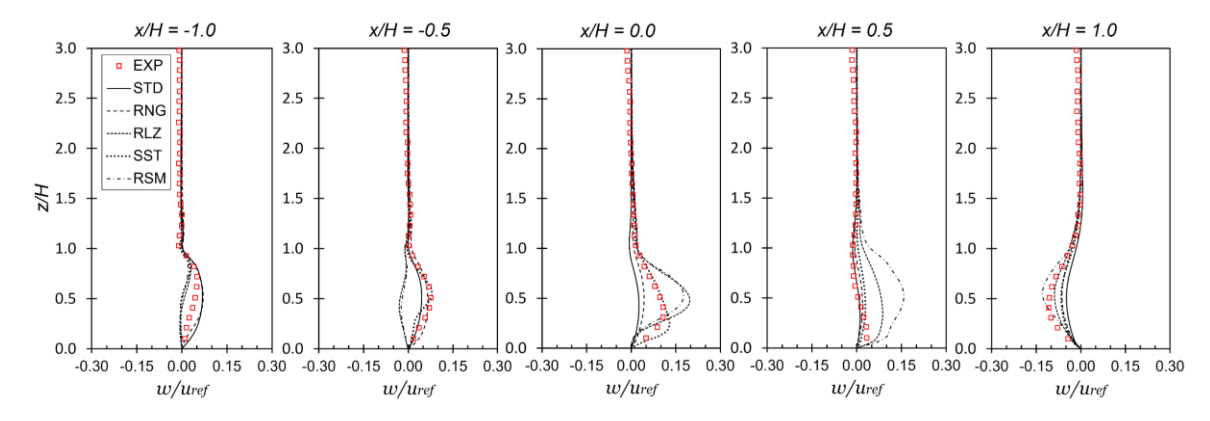


Figure 7. Comparison of dimensionless mean vertical velocity (w/u_{ref}) obtained from RANS simulations of various closure models with wind-tunnel results along three vertical lines of the target canyon at (a) x/H = 1.0, (b) x/H = 0.0, and (c) x/H = 1.0.

3.2.3 Validation Metrics

To obtain a comprehensive and quantitative evaluation of the performance of all five closure models, two validation metrics are employed; the factor of 2 of the observations (FAC2) and the factor of 1.3 of the observations (FAC1.3) for the streamwise and vertical velocities. Both metrics are calculated using Eq. (2) and Eq. (3):

$$FAC2 = \frac{1}{N} \sum_{i=1}^{n} N_i \text{ with } N_i = \begin{cases} 1 \text{ for } 0.5 \le \frac{P_i}{O_i} \le 2\\ 0 \text{ else} \end{cases}$$
 (2)

$$FAC1.3 = \frac{1}{N} \sum_{i=1}^{n} N_i \text{ with } N_i = \begin{cases} 1 \text{ for } 0.77 \le \frac{P_i}{O_i} \le 1.3 \\ 0 \text{ else} \end{cases}$$
 (3)

where P_i represents the predicted value using CFD, O_i is the observed value obtained from experiments, and N indicates the total number of measurement points (29 points × 5 lines = 145). The threshold value for the FAC2 is set to FAC2 > 0.5 [24,38–40]. Findings for both metrics are summarized in Table 1. All FAC values for u/u_{ref} are higher than the threshold value of 0.5, indicating that all closure models accurately estimate streamwise velocity. RNG surpasses all models with a FAC2 of 0.92, followed by STD at 0.91, while the remaining three models (RLZ, SST, and RSM) each acquire a value of 0.88, 0.89 and 0.90, respectively. In the FAC1.3 calculations, RNG maintains to demonstrate the best performance, followed by SST, while STD and RLZ perform equally, followed by RSM. The majority of the compared data concentrated within the 10% error, demonstrating the models' consistency in forecasting the streamwise velocity as shown in Figure 8(a).

The measurement of the vertical velocity (w/u_{ref}) produces the highest FAC2 of RNG (0.38), followed by SST (0.34), STD (0.21), and RSM (0.20), with RLZ obtaining the lowest value of 0.19. In the FAC1.3 evaluation, the top three rankings remain corresponding to FAC2, but the lowest two models exhibit an identical value of 0.04. These findings indicate that all models encounter difficulties in predicting vertical velocity, as the FAC2 values are below the threshold of 0.5. Figure 8(b) clearly illustrates that the data demonstrate scattering around the diagonal lines, indicating large disparities.

Table 1: Validation metrics for dimensionless streamline velocities (u/u_{ref}) and vertical velocities (w/u_{ref})	_f):
FAC2: factor of two observations; FAC1.3: factor of 1.3 observations	

Turbulence model -	u/u_{ref}		w/u_{ref}	
	FAC2	FAC1.3	FAC2	FAC1.3
STD	0.91	0.81	0.21	0.07
RNG	0.92	0.81	0.38	0.17
RLZ	0.88	0.82	0.19	0.04
SST	0.89	0.81	0.34	0.13
RSM	0.90	0.79	0.20	0.07
Ideal	1	1	1	1

3.2.4 Velocity Contour Plot

Figure 9 displays the dimensionless streamwise velocity contour for the experiment as a reference and all closure models over the x-z plane at y/H = 0.0. Please note that the horizontal axis (x/H) values for EXP differ from the simulations since these values are derived directly from the experimental results without any adjustments to align with the simulation axis (see Figure 9(a)). The EXP clearly demonstrates the development of two counterrotating vortices, with the primary vortex encompassing a substantial portion of the canyon width, exhibiting a distorted configuration on the upstream side, while a secondary counter-clockwise vortex is observed adjacent to the leeward wall, confirming several previous investigations for the wake interference flow regime [4,24,36]. The primary vortex for STD is more evenly distributed throughout the canyon, except for a minor counterclockwise vortex at the lower corner of the leeward wall. The flow structure predicted by the RNG successfully represents the wake interference, which is qualitatively comparable to the EXP. On the other hand, the RLZ shows three vortices with a skimming-like flow in the half-width of the canyon downstream. Additionally, in the upstream region, two nearly triangular-shaped counter-rotating vortices are observed. For the SST, the in-canyon flow is

further modified, leading to the formation of the primary vortex, characterized by a more horizontally distributed reverse flow in the upper half of the canyon height within the upstream region. A horizontally extended secondary vortex forms adjacent to the leeward wall. The flow structure of the RSM is very similar to that of the SST, differing primarily through the presence of four vortices due to modifications in the flow within the lower half of the canyon height near the upstream area. The three models RLZ, SST, and RSM are clearly insufficient in replicating the wake interference flow regime in comparison to the EXP.

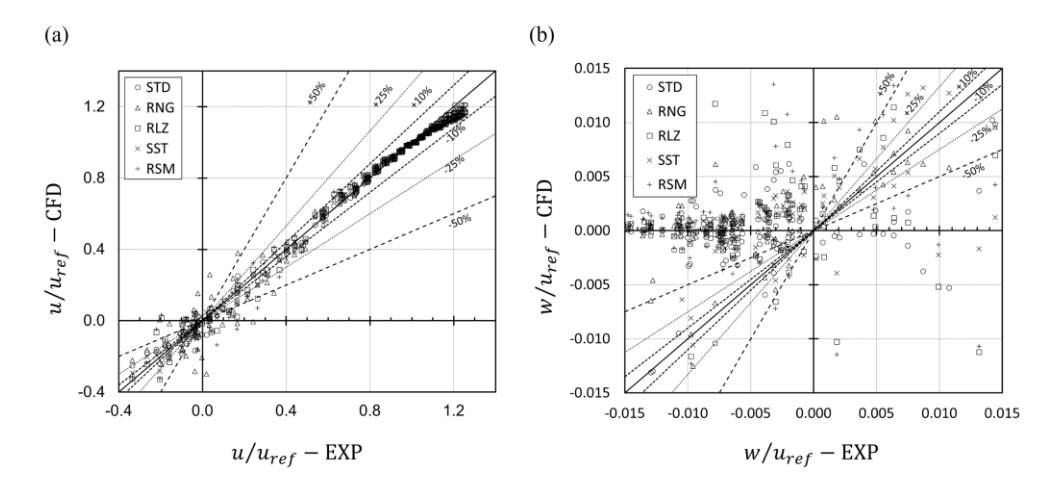


Figure 8. Comparison of (a) streamwise and (b) vertical velocities between CFD and experimental (EXP) data across three vertical lines.

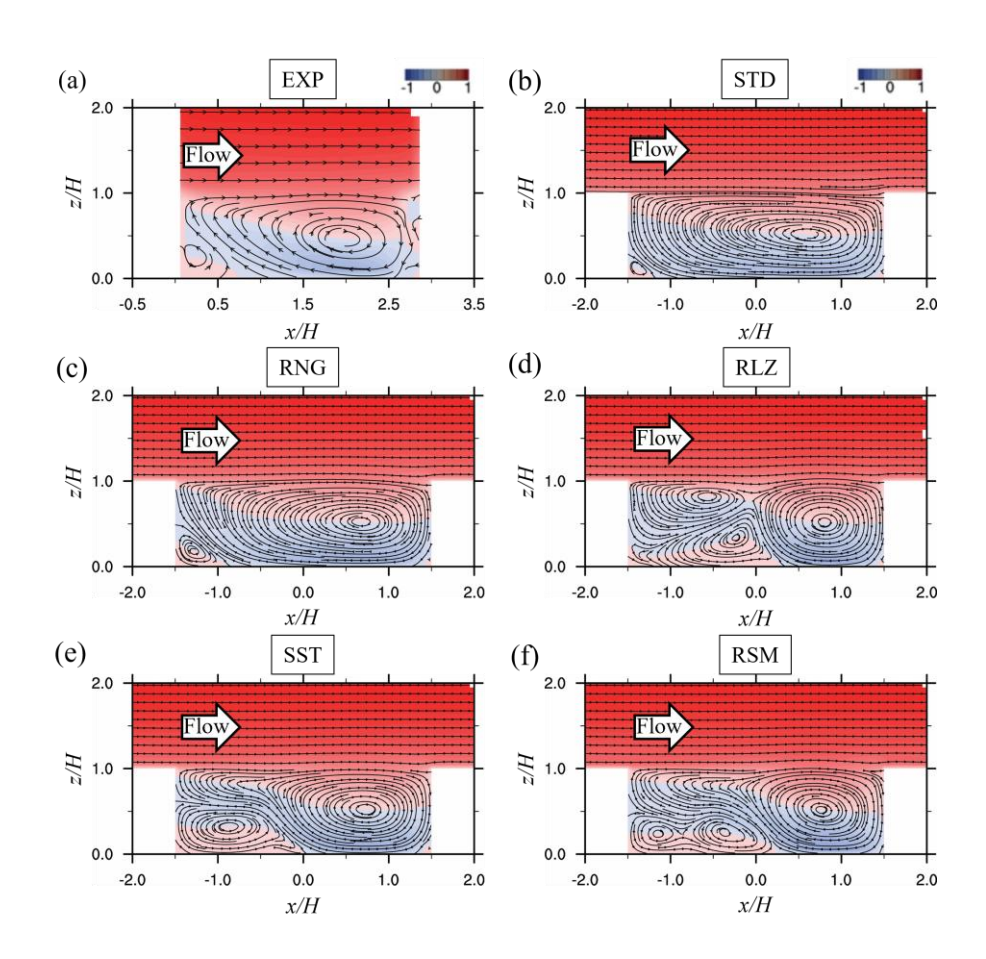


Figure 9. Dimensionless streamwise velocity contours (a) EXP (b) STD (c) RNG (d) RLZ (e) SST (f) RSM.

4.0 CONCLUSION

The present investigation performs a series of CFD simulations using steady RANS equations to assess the efficacy of different turbulence closure models. Five closure models are assessed: STD, RNG, RLZ, SST, and RSM, throughout the wake interference flow regime structure of a 2D street canyon with an aspect ratio S/H = 3. The main conclusions of this study are presented as follows:

- All models demonstrate an excellent ability for predicting the streamwise velocity within the canyon, as the FAC2 values exceed the threshold of 0.5. The RNG model (0.92) surpasses other models, followed by STD (0.91), RSM (0.90), SST (0.89), and RLZ (0.88).
- None of the evaluated models adequately predicted the in-canyon vertical velocity, since all FAC2 values fell below the threshold. This clearly demonstrates the limitations of RANS models in predicting lowmomentum fluid regions.
- The streamlines of the streamwise and vertical components depicted diverse in-canyon flow patterns governed by the evaluated models. Both RNG and STD exhibit behaviour almost identical to the EXP, which distinctly predicts the wake interference flow pattern characterized by a primary vortex that occupies a significant portion of the canyon width, along with the formation of a counter-rotating vortex near the leeward corner. Both models illustrate smaller diffusion resulting in larger recirculation flow compared to the experimental results. Nevertheless, other models exhibit insufficient performance in predicting the flow pattern.

ACKNOWLEDGEMENT

The study was conducted at the computer lab of Wind Engineering & Building Physics (WEBP), Faculty of Mechanical Engineering, Universiti Teknologi MARA, Shah Alam, Malaysia.

AUTHORS CONTRIBUTION

Mohd Hilman Mohd Akil Tan: Formal analysis, Investigation, Methodology, Validation, Writing - Original Draft Mohd Faizal Mohamad: Supervision, Conceptualization, Methodology, Writing - Review & Editing, Resources. Azli Abd Razak: Supervision, Writing - Review & Editing

Nurnida Elmira Othman: Writing - Review & Editing

Shahliza Azreen Sarmin: Writing - Review & Editing

DECLARATION OF COMPETING OF INTEREST

The authors declare that they have no known competing financial interests or personal relationships that could have appeared to influence the work reported in this paper.

REFERENCES

- [1] J. Hang, X. Chen, G. Chen, T. Chen, Y. Lin, Z. Luo, X. Zhang, Q. Wang, The influence of aspect ratios and wall heating conditions on flow and passive pollutant exposure in 2D typical street canyons, Build Environ 168 (2020). https://doi.org/10.1016/j.buildenv.2019.106536.
- [2] Y. dong Huang, C. Long, J. tong Deng, C.N. Kim, Impacts of Upstream Building Width and Upwind Building Arrangements on Airflow and Pollutant Dispersion in a Street Canyon, Environ Forensics 15 (2014) 25–36. https://doi.org/10.1080/15275922.2013.872714.
- [3] T.N.H. Chung, C.H. Liu, On the Mechanism of Air Pollutant Removal in Two-Dimensional Idealized Street Canyons: A Large-Eddy Simulation Approach, Boundary Layer Meteorol 148 (2013) 241–253. https://doi.org/10.1007/s10546-013-9811-4.
- [4] T.R. Oke, Street Design and Urban Canopy Layer Climate, 1988.
- [5] J. Hang, L. Chen, Y. Lin, R. Buccolieri, B. Lin, The impact of semi-open settings on ventilation in idealized building arrays, Urban Clim 25 (2018) 196–217. https://doi.org/10.1016/j.uclim.2018.07.003.
- [6] M.F. Ibrahim, M.F. Mohamad, N. Ikegaya, A.A. Razak, Numerical Investigation of Flow and Dispersion over Two-Dimensional Semi-Open Street Canyon, CFD Letters 15 (2023) 53–70. https://doi.org/10.37934/cfdl.15.2.5370.
- [7] X. Zheng, H. Montazeri, B. Blocken, Impact of building façade geometrical details on pollutant dispersion in street canyons, Build Environ 212 (2022). https://doi.org/10.1016/j.buildenv.2021.108746.
- [8] M.G. Badas, M. Garau, G. Querzoli, How gable roofs change the mechanisms of turbulent vertical momentum transfer: A LES study on two-dimensional urban canyons, Journal of Wind Engineering and Industrial Aerodynamics 209 (2021). https://doi.org/10.1016/j.jweia.2020.104432.

- [9] M.G. Badas, S. Ferrari, M. Garau, G. Querzoli, On the effect of gable roof on natural ventilation in two-dimensional urban canyons, Journal of Wind Engineering and Industrial Aerodynamics 162 (2017) 24–34. https://doi.org/10.1016/j.jweia.2017.01.006.
- [10] S. Ferrari, M.G. Badas, M. Garau, A. Seoni, G. Querzoli, The air quality in narrow two-dimensional urban canyons with pitched and flat roof buildings, Int. J. Environment and Pollution 62 (2017) 347–368.
- [11] A.A. Aliabadi, E.S. Krayenhoff, N. Nazarian, L.W. Chew, P.R. Armstrong, A. Afshari, L.K. Norford, Effects of Roof-Edge Roughness on Air Temperature and Pollutant Concentration in Urban Canyons, Boundary Layer Meteorol 164 (2017) 249–279. https://doi.org/10.1007/s10546-017-0246-1.
- [12] R. Kellnerová, L. Kukačka, K. Jurčáková, V. Uruba, Z. Jaňour, PIV measurement of turbulent flow within a street canyon: Detection of coherent motion, Journal of Wind Engineering and Industrial Aerodynamics 104–106 (2012) 302–313. https://doi.org/10.1016/j.jweia.2012.02.017.
- [13] R. Kellnerová, V. Fuka, V. Uruba, K. Jurčáková, Š. Nosek, H. Chaloupecká, Z. Jaňour, On street-canyon flow dynamics: Advanced validation of LES by time-resolved PIV, Atmosphere (Basel) 9 (2018). https://doi.org/10.3390/atmos9050161.
- [14] Y. Zhao, H. Li, A. Kubilay, J. Carmeliet, Buoyancy effects on the flows around flat and steep street canyons in simplified urban settings subject to a neutral approaching boundary layer: Wind tunnel PIV measurements, Science of the Total Environment 797 (2021). https://doi.org/10.1016/j.scitotenv.2021.149067.
- [15] Y. Luo, Z. Yin, Q. Liang, C. Yao, C. Bao, Y. Wu, Y. Huang, Effects of tree characteristics and arcade design on the traffic pollutant dispersion inside the asymmetric street canyon, Sustain Cities Soc 122 (2025). https://doi.org/10.1016/j.scs.2025.106244.
- [16] N. Mishra, A.K. Patra, A. Penchala, S. Santra, Numerical investigation of the influence of street length and building configurations on ventilation and pollutant dispersion in idealized street canyons, Journal of Wind Engineering and Industrial Aerodynamics 257 (2025). https://doi.org/10.1016/j.jweia.2025.106016.
- [17] Y. Wang, K. Zhong, J. He, J. Cheng, M. Qi, Y. Kang, Impacts of pollution from surrounding street canyons on air cleanliness in urban ventilation corridors, Sustain Cities Soc 130 (2025). https://doi.org/10.1016/j.scs.2025.106552.
- [18] S.M. Salim, R. Buccolieri, A. Chan, S. Di Sabatino, Numerical simulation of atmospheric pollutant dispersion in an urban street canyon: Comparison between RANS and LES, Journal of Wind Engineering and Industrial Aerodynamics 99 (2011) 103–113. https://doi.org/10.1016/j.jweia.2010.12.002.
- [19] Y. Huang, X. Hu, N. Zeng, Impact of wedge-shaped roofs on airflow and pollutant dispersion inside urban street canyons, Build Environ 44 (2009) 2335–2347. https://doi.org/10.1016/j.buildenv.2009.03.024.
- [20] Y.K. Ho, C.H. Liu, M.S. Wong, Preliminary study of the parameterisation of street-level ventilation in idealised two-dimensional simulations, Build Environ 89 (2015) 345–355. https://doi.org/10.1016/j.buildenv.2015.02.042.
- [21] P. Qin, A. Ricci, B. Blocken, On the accuracy of idealized sources in CFD simulations of pollutant dispersion in an urban street canyon, Build Environ 265 (2024). https://doi.org/10.1016/j.buildenv.2024.111950.
- [22] M.F. Ibrahim, M.F. Mohamad, N. Ikegaya, A. Abd Razak, Numerical Investigation on the Effect of Building Overhang on the Flow within Idealised Two-dimensional Street Canyon, ESTEEM Academic Journal 17 (2021) 67–77.
- [23] W.C. Cheng, C.H. Liu, Large-Eddy Simulation of Flow and Pollutant Transports in and Above Two-Dimensional Idealized Street Canyons, Boundary Layer Meteorol 139 (2011) 411–437. https://doi.org/10.1007/s10546-010-9584-y.
- [24] A. Alwi, M.F. Mohamad, N. Ikegaya, A.A. Razak, Effect of protruding eave on the turbulence structures over two-dimensional semi-open street canyon, Build Environ 228 (2023). https://doi.org/10.1016/j.buildenv.2022.109921.
- [25] M.F. Mohamad, A. Hagishima, N. Ikegaya, J. Tanimoto, A.R. Omar, Aerodynamic effect of overhang on a turbulent flow field within a two-dimensional street canyon, 2015.
- [26] Y. Tominaga, A. Mochida, R. Yoshie, H. Kataoka, T. Nozu, M. Yoshikawa, T. Shirasawa, AIJ guidelines for practical applications of CFD to pedestrian wind environment around buildings, Journal of Wind Engineering and Industrial Aerodynamics 96 (2008) 1749–1761. https://doi.org/10.1016/j.jweia.2008.02.058.
- [27] J. Franke, A. Hellsten, H. Schlünzen, B. Carissimo, Best Practice Guideline for the CFD Simulation of Flows in the Urban Environment: COST Action 732 Quality Assurance and Improvement of Microscale Meteorological Models, University of Hamburg, 2007.
- [28] OpenCFD, OpenFOAM, (2023). https://www.openfoam.com/ (accessed September 13, 2023).
- [29] B.E. Launder, D.B. Spalding, THE NUMERICAL COMPUTATION OF TURBULENT FLOWS, 1974.

- [30] V. Yakhot, S.A. Orszag, S. Thangam, T.B. Gatski, C.G. Speziale, Development of turbulence models for shear flows by a double expansion technique, Physics of Fluids A 4 (1992) 1510–1520. https://doi.org/10.1063/1.858424.
- [31] T.-H. Shih, W.W. Liou, A. Shabbir, Z. Yang, J. Zhu, A NEW k-ε EDDY VISCOSITY MODEL FOR HIGH REYNOLDS NUMBER TURBULENT FLOWS, 1995.
- [32] F.R. Menter, Two-equation eddy-viscosity turbulence models for engineering applications, AIAA Journal 32 (1994) 1598–1605. https://doi.org/10.2514/3.12149.
- [33] K. Hanjalic, K. Hanjalic, B.E. Launder, Hanjalic-Launder JFM Vol52 1972 A Reynolds stress model of turbulence and its application to thin shear flows, 1972.
- [34] Y. Tominaga, A. Mochida, R. Yoshie, H. Kataoka, T. Nozu, M. Yoshikawa, T. Shirasawa, AIJ guidelines for practical applications of CFD to pedestrian wind environment around buildings, Journal of Wind Engineering and Industrial Aerodynamics 96 (2008) 1749–1761. https://doi.org/10.1016/j.jweia.2008.02.058.
- [35] P.J. Roache, Quantification of uncertainty in computational fluid dynamics, Annu. Rev. Fluid. Mech 29 (1997) 123–160. www.annualreviews.org.
- [36] T. Sato, A. Hagishima, N. Ikegaya, J. Tanimoto, Wind tunnel experiment on turbulent flow field around 2D street canyon with eaves, Journal of Environmental Engineering (Japan) 81 (2016) 467–476. https://doi.org/10.3130/aije.81.467.
- [37] Y. Tominaga, T. Stathopoulos, CFD modeling of pollution dispersion in a street canyon: Comparison between LES and RANS, Journal of Wind Engineering and Industrial Aerodynamics 99 (2011) 340–348. https://doi.org/10.1016/j.jweia.2010.12.005.
- [38] K. Nakajima, R. Ooka, H. Kikumoto, Evaluation of k-ε Reynolds stress modeling in an idealized urban canyon using LES, Journal of Wind Engineering and Industrial Aerodynamics 175 (2018) 213–228. https://doi.org/10.1016/j.jweia.2018.01.034.
- [39] S.R. Hanna, O.R. Hansen, S. Dharmavaram, FLACS CFD air quality model performance evaluation with Kit Fox, MUST, Prairie Grass, and EMU observations, Atmos Environ 38 (2004) 4675–4687. https://doi.org/10.1016/j.atmosenv.2004.05.041.
- [40] D. Hertwig, G.C. Efthimiou, J.G. Bartzis, B. Leitl, CFD-RANS model validation of turbulent flow in a semi-idealized urban canopy, Journal of Wind Engineering and Industrial Aerodynamics 111 (2012) 61–72. https://doi.org/10.1016/j.jweia.2012.09.003.